

MCEN90032 Sensor Systems - Workshop 2

Indoor GPS

Tuan Khoi Nguyen (1025294)

Introduction

This report will demonstrate the process of developing measurements from MATLAB Mobile Phone Sensors into an indoor GPS, which can be divided into 2 parts: walking distance estimation, heading estimation. For walking distance, 2 estimation methods will be computed and compared together: the constant step assumption and integral approximation. For heading estimation, the outcome will be calculated using sensor fusion of both signals through Kalman Filter. The indoor GPS output, as a result of combining both processes, will be demonstrated in the results section, where its strengths and weaknesses will be evaluated, and further improvement ideas will be applied.

Key goals

The report will include the following listed:

- Setting up and define initial measurement parameters.
- Calibration of the sensor to detect bias and uncertainty variables.
- Extension of step counter into walking distance estimation, using 2 different methods.
- The process of getting heading estimation from magnetometer and gyroscope.
- The methodology of fusing the heading estimations using Kalman Filter.
- Display and demonstration of combining distance and heading estimations to determine the overall path.
- Evaluations of outputs and improvement suggestions.
- Method appendix: all the evaluation or theories that aids in developing the methodologies.

Terminologies & Credentials

In this report, a number of the following terminologies will be used:

- Google Maps Coordinate (GC): Reference system used by Google Maps. The path plots will use this map as covering background, which was already included with a distance scale conversion to meters. The 2D origin of reference will be set to the starting point of recording.
- Compass Coordinate (CC): Reference system used in compasses. This is also the coordinate system used in the heading estimations from the sensor data.

Stage 1

Settings

This stage describes how the recording process is done to ensure that correct and meaningful data is retrieved.

1.1 Orientation & Path

In this experiment, the user will initially face 35 degrees anti-clockwise from the East direction. For measurement simplicity, the main user will hold the phone screen pointing up, with the phone's top heading towards left direction of user. That way, the expected true values of the orientation in (Azimuth, Pitch, Roll) in GC will respectively be $(35^\circ, 0^\circ, 0^\circ)$. For the path taken, to be similar to the length of an indoor walk, the user will take a clockwise-cyclic and triangular path that will result in approximately 100 meters of walking.

1.2 Sampling Rate

Being an extension from the step counting algorithm, the sampling rate is set to remain the same at 10Hz. As mentioned in the previous development of the pedometer, this is because a safe upper bound on the average walking pace is 5Hz, and the Shannon-Nyquist theorem requires a sampling rate at least twice the signal frequency to capture its details, making 10Hz the best choice to capture enough information while not letting too much noise get in.

1.3 Recording Processes

The process will begin with 5 seconds of standing still, then user will walk at constant speed and heading for at least 10 seconds. This will be the calibration stage of the process. While walking, the user will take 2 turns, and will eventually reach the starting destination to create a cyclic and triangular path. For validation purposes, when stopping, the user is assumed to be fully stationary - not taking any turns as well.

With these steps, acceleration, magnetic field from magnetometer, and angular velocity from gyroscope will be recorded while walking.

1.4 Initial Overview

A path plot in Figure 1.1 is shown to demonstrate the walked route, along with the recorded GPS.

As seen in the comparison above, the GPS seems not to reflecting the true path. This shows that the GPS have a high error margin, and may not be suitable to measure close distances like indoor paths. This proves that a development for an indoor GPS is needed, which is the purpose of this report.

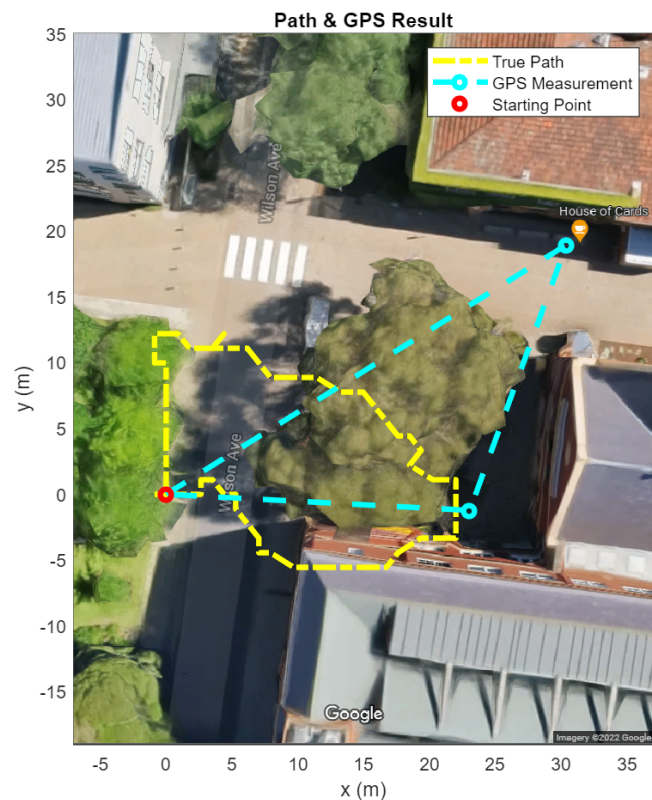


Figure 1.1: The true walking path (clockwise) of the user and its GPS measurement

Stage 2

Walking Distance Estimation

To first develop the indoor GPS, the step counter from previous work, which has included noise filtering and peak detection functionalities, will be extended into a walking distance estimator using its outputs. 2 different extraction methods will be used to extend the steps: a range-based method and a stride-based method.

2.1 Summary of Pedometer Algorithm

The pedometer only uses the acceleration data to process.

Calibration First, it will use Linear Regression to measure the bias and calibrate the sensor, then retrieve the norm of the acceleration.

Frequency analysis & Noise filtering The norm is then put through Fourier Transform to get the frequency strengths, which will be fitted with a bell curve and applied the 3-sigma rule to find the suitable thresholds for the bandpass filtering.

Peak finding After filtering, the signal will try and detect peaks that exceeds a requirement height (below the noise retrieved from calibration) and has a reasonable period as a step duration.

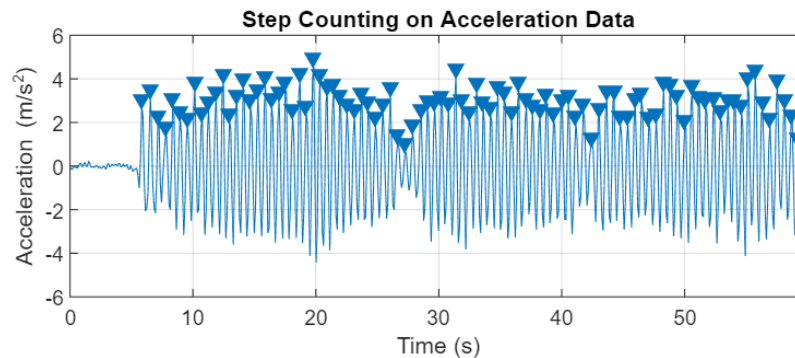


Figure 2.1: Result of applying the Step Counting algorithm from previous development to the current walking data. Each triangle denotes a peak, where a step is taken

In the next sections, 2 different methods will be introduced to further process the step counting results.

2.2 Constant Step Estimation (CSE)

As the name suggests, this method assumes a constant stride of the user when walking, which before the experiment was roughly measured to be 0.65 meters. However, just assuming so would cause inaccurate reflection when the user is stopping, and produce wrong measurement as a result.

Therefore, the method will also attempt to detect stopping ranges by looking at the time difference between 2 consecutive steps. Given from the pedometer development, a lower bound for walking frequency is 1Hz, hence 1 seconds without steps is set as the minimum duration to be considered a stopping period.

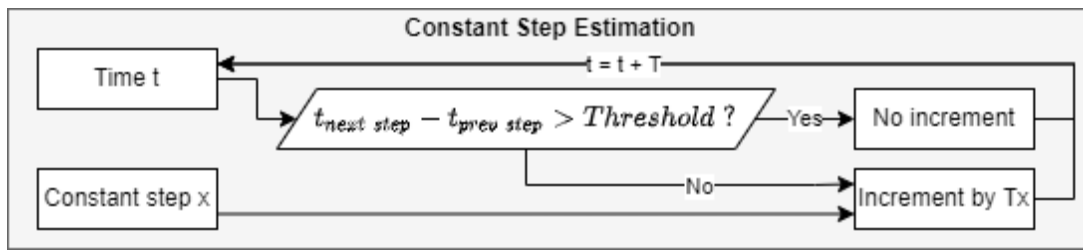


Figure 2.2: Algorithm flowchart for CSE

2.3 Approximated Stride Estimation (ASE)

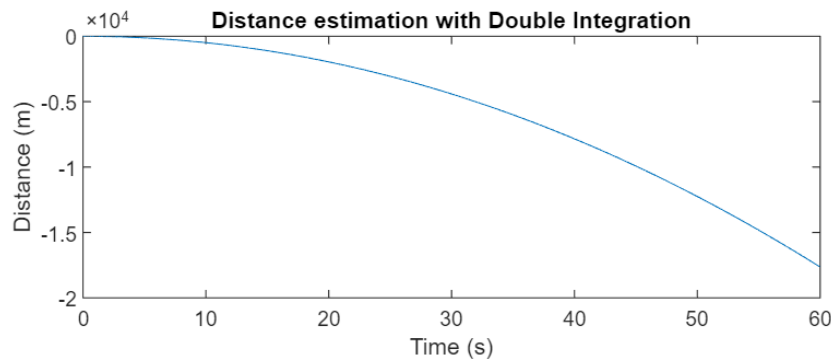


Figure 2.3: Distance estimation using double integration from acceleration data

In reality, the user will actually have fluctuations in their speed, which is not constant. Theoretically, given acceleration, the distance can be estimated using double integration. However, with drift occurring in acceleration, which through double integration will be squared up, the result returned will not be reliable, as shown in Figure 2.3.

Therefore, a step-by-step approximation method is used instead to estimate the length of each stride, using the common formula $x = (v_0 + v)t$ and the peak information from pedometer output:

- v is approximated using integration of a half-sine wave that matches the peak.
- v_0 is linearly approximated using the peak magnitudes.

More mathematical details, consisting of assumptions and proof, will be described in Appendix A.2.

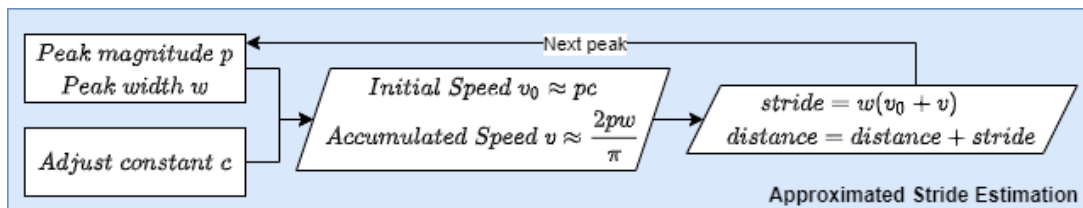


Figure 2.4: Algorithm flowchart for ASE

Stage 3

Heading Estimation

Other than distance, turns also need to be detected in order to make a complete route. Therefore, the heading of the route is estimated. Using an internal measurement unit, there are 2 possible inputs that can be converted into orientation: the magnetic field and angular velocity. To limit down the noise and retrieve a more reflective signal, the raw signals are put through a low-pass filter that eliminates the signals that exceed the sampling rate.

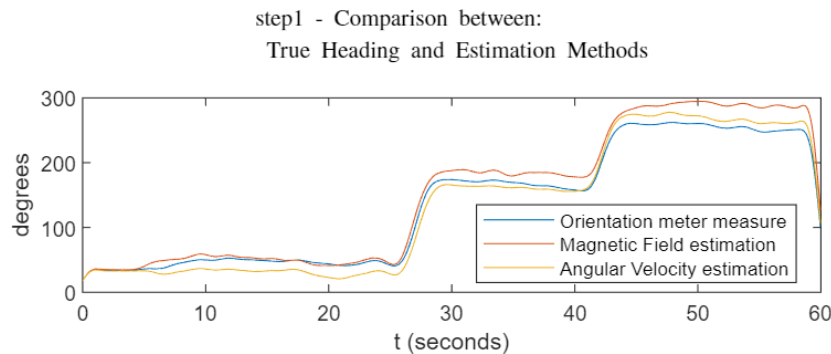


Figure 3.1: Initial heading estimation using different measurements. Tilt compensation applied for gyroscope.

3.1 Magnetometer Estimation

Magnetometer measures the magnetic field \mathbf{h} between the device and the Earth as a 3-dimensional vector in CC, and is therefore dependent on the orientation of the phone positioning. For the user's phone position, the z-axis of the vector will point down towards the Earth center [1], and the 2D orientation, represented as the clockwise angle from the North direction, can be calculated as $-\tan(h_y/h_x)$.

However, the measurement can be easily affected by magnetic or metal sources nearby, which are known as the soft iron (causing offsets from the origin) and hard iron effects (causing ellipsoid distribution of the vectors) [2]. Even though the effect can be calibrated by reshaping the distribution to a sphere with center at origin, there is no guarantee that this will reduce the effect fully, given that various magnetic sources or metal objects can unknowingly appear during recording. Therefore, it is suitable to combine the heading estimation of magnetometer with another estimation that is not affected by magnetic factors.

3.2 Gyroscope Estimation

Gyroscope measures the relative angular velocity of the object in 3 dimensions in CC, where in the user's position, the positive direction is a clockwise turn. The orientation can be estimated by cumulatively adding up the angular velocity measurement. However, similar to the acceleration sensor, drifting can happen, which causes the estimated heading to increase or decrease gradually from the correct result, as shown in the final third of the signal in Figure 3.1.

Tilt compensation One common way to correct the drifting of the gyroscope is to force setting the measurement to 0 if the user is detected to be stopping - having assumed to be fully stationary, which is already done during constant step estimation for walking distance. While the correction does show a better reflective value during stopping time (first 5 seconds in Figure 3.1), drifting would still happen during walking, which the true value would not be known.

It is feasible to combine the gyroscope estimation with a non-integral estimation that is not affected by drifting. With the magnetometer measurement retrieved, Kalman Filter can be used to combine the measurements together and get a more suitable estimation of the true heading.

3.3 Calibration

Both signals will be calibrated when standing still and when moving at constant speed. This way, the bias can be detected and removed the same way as acceleration data with Linear Regression. Furthermore, the variance of the heading estimations or angular velocity will also be recorded for Kalman Filter inputting.

3.4 Kalman Filter

3.4.1 State Representation & Algorithm

The Kalman Filter [3] aims to balance between prediction and measurement to give out the best possible estimation of the next state \mathbf{x} and its covariance \mathbf{P} , using the variable \mathbf{K} . To aid this process, \mathbf{Q} and \mathbf{R} , the respective covariance matrices of the noise vectors \mathbf{w} and \mathbf{v} , are needed.

To apply the filter, a state representation in the following form is needed:

$$\begin{cases} \mathbf{x}_{k+1} = \mathbf{F}\mathbf{x}_k + \mathbf{w}_k \\ \mathbf{z}_{k+1} = \mathbf{H}\mathbf{x}_k + \mathbf{v}_k \end{cases}$$

Where \mathbf{x} is a vector of state variables, \mathbf{F} being the transition matrix that maps the current state to the next state, and \mathbf{w} being the process noise. Vector \mathbf{z} denotes the measurement of interest, which can be retrieved from \mathbf{x} with the observation matrix \mathbf{H} . The noise of this process is denoted by the vector \mathbf{v} . The next section will describe how the state model is developed along with the variables of interest, as well as the reasoning of choice for the initial guesses.

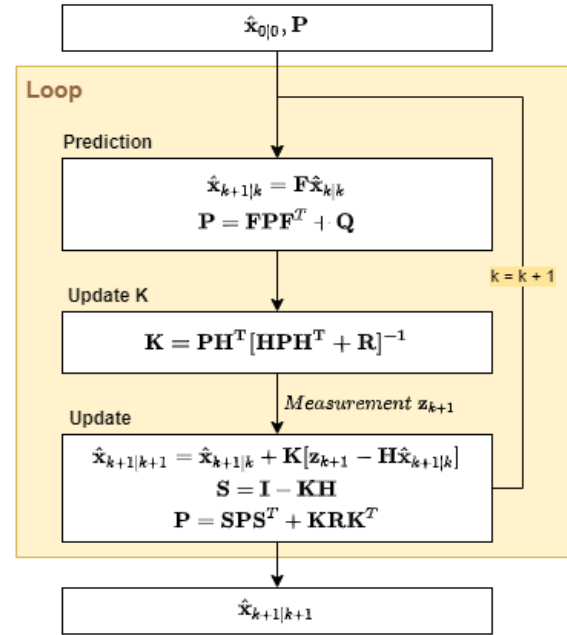


Figure 3.2: Algorithm flowchart of Kalman Filter, adapted from Kaniewski and Kazubek [1]

3.4.2 State Variables

Given the magnetometer and the gyroscope, the following variables of interest can be put into the state vector:

- θ : The relative clockwise rotation angle from the initial heading. Measurement of this variable can be taken from the heading estimation of the magnetometer.
- $\dot{\theta}$: The angular velocity of the object, which can be measured directly from the gyroscope.

As mentioned, sampling frequency of 10Hz is chosen to capture the most information without letting too much noise getting in. With the sampling frequency f known, along with the discrete formula $\theta = \theta_0 + T\dot{\theta}$, the following matrix equation can be formed, which gives the transition matrix \mathbf{F} :

$$\begin{bmatrix} \theta_{k+1} \\ \dot{\theta}_{k+1} \end{bmatrix} = \begin{bmatrix} 1 & 1/f \\ 0 & 1 \end{bmatrix} \begin{bmatrix} \theta_k \\ \dot{\theta}_k \end{bmatrix} \rightarrow \mathbf{F} = \begin{bmatrix} 1 & 1/f \\ 0 & 1 \end{bmatrix}$$

And with the measurement of interest being the first variable in the state vector, the observation matrix will then be $\mathbf{H} = [1 \ 0]$. These details also show that the system is fully observable.

With calibration removing bias and user standing still at origin initially, the initial state can be ensured to be $\begin{bmatrix} \theta_0 \\ \dot{\theta}_0 \end{bmatrix} = \begin{bmatrix} 0^\circ \\ 0^\circ \end{bmatrix}$, which satisfies the assumptions of the **initial state being zero-mean** and **independent to the random process noises**.

3.4.3 Uncertainty Variables

In this task, the sensor process noise will be assumed to be **Gaussian white**. By walking constantly during calibration time, through fitting a normal distribution to the signal, standard deviations for both signals are retrieved: σ_m for magnetometer heading and σ_g for gyroscope angular velocity. As $\mathbf{w}(k)$ comes from the magnetometer, the measurement covariance becomes a scalar denoting its variance: $\mathbf{R} = \sigma_m^2$.

As the measurements of magnetometer and gyroscope, which corresponds to $\mathbf{w}(k)$ and $\mathbf{v}(k)$ respectively, are coming from 2 different sensors, the assumption of $\mathbf{w}(k)$ and $\mathbf{v}(k)$ being **2 independent processes** is satisfied. This also makes the covariance between 2 state variables become 0, and the process covariance matrix becomes $\mathbf{Q} = \begin{bmatrix} \sigma_m^2 & 0 \\ 0 & \sigma_g^2 \end{bmatrix}$. And as the initial position is set up and ensured, the initial covariance matrix will also have no noise: $\mathbf{P}_0 = [0]$.

3.5 Fusion Results

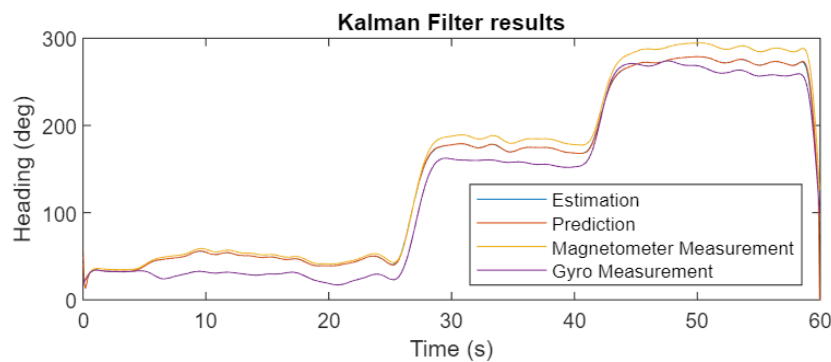


Figure 3.3: Result of implementing the Kalman Filter

The result from Figure 3.3 shows that the Kalman Filter's estimated heading is a well combination between the 2 heading estimations, having mostly lower values than the magnetometer, and no drifting like the gyroscope measurement. The heading estimation is now ready to be combined with the walking distance estimation.

3.6 Combination to Indoor GPS

3.6.1 Remapping CC to GC

It is noticeable that the estimated route will be in GC, where the positive x-axis points to the East, the positive y-axis points to the North and the positive z-axis points upwards. However, the heading estimate is in CC, where the positive x-axis points to the North, the positive y-axis points to the East and the positive z-axis pointing down. Therefore, mapping method is needed to rotate the estimations from CC to GC. The full form of the matrix will be shown in Appendix A.3, which performs the following actions:

- Flip the z-axis over by rotating 180° around the y-axis.
- Reposition x and y axes by rotating 90° around the z-axis.

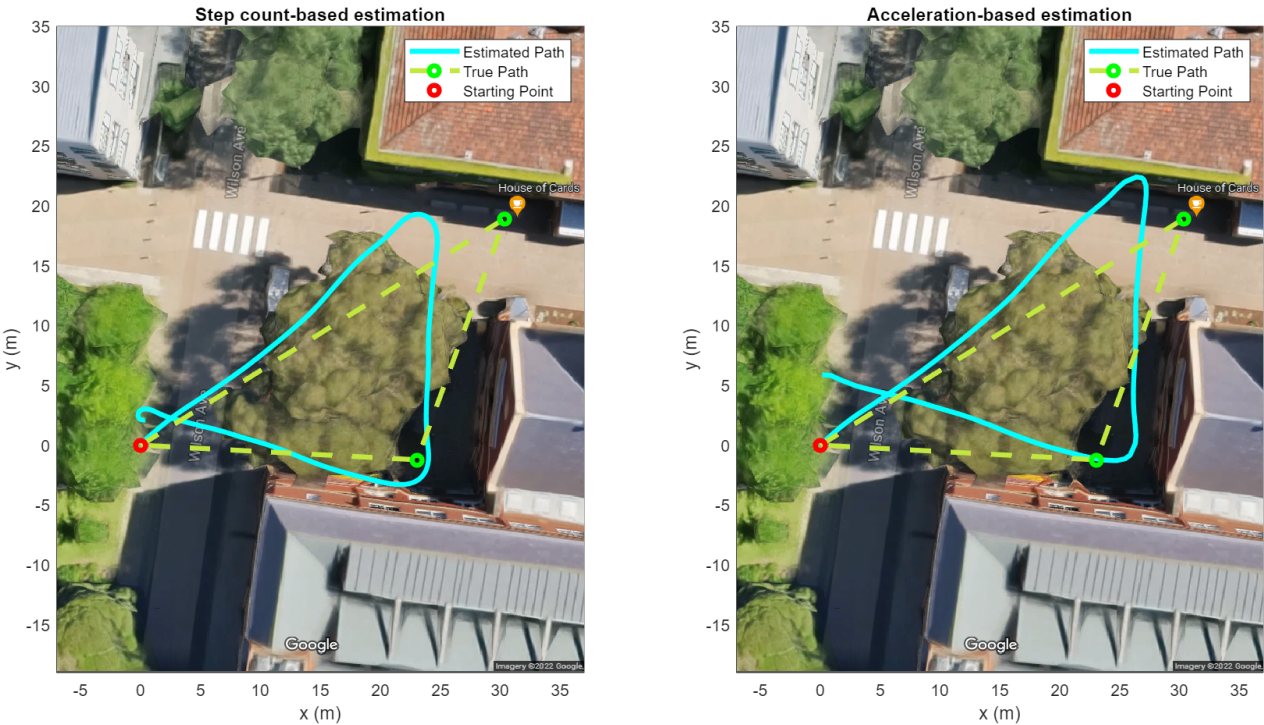
3.6.2 Incremental Method

With 2 distance estimation methods operating differently, how they are fused with the heading estimation θ is also different. The same procedure is that the unit displacement will now be separated into x and y Cartesian components in GC, given the polar representation, using trigonometry conversion $Cartesian(u, \theta) = [u \cos(\theta) \ u \sin(\theta)]$:

- CSE with constant stride s at time t and sampling frequency f : Same incremental algorithm, which does not increment if user is detected stopping, and increment by $Cartesian(s/f, \theta(t))$ otherwise.
- ASE: For each step detected at time t , get the corresponding stride s and heading estimation $\theta(t)$. The increment will then be $Cartesian(s, \theta(t))$.

Stage 4

Results & Analysis



(a) Estimated path of the user, using CSE (b) Estimated path of the user, using ASE

Figure 4.1: The ground truth compared with indoor GPS methods

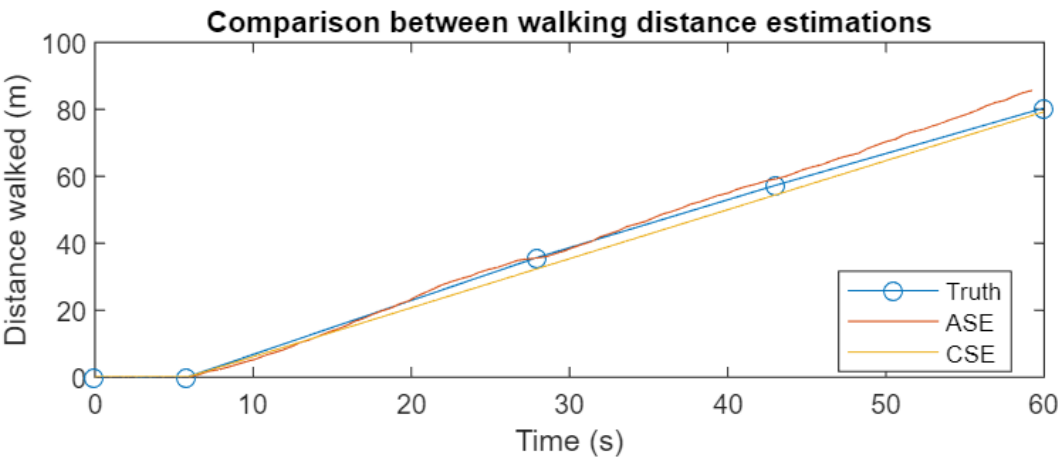


Figure 4.2: Comparison between 2 distance estimation methods

4.1 Evaluation

The evaluation part will look at different sections of the walking route, to see how well each algorithm performs in different scenarios of walking. The main sections of interest are straight paths, turns, and a small turn made at the end of the path.

4.1.1 CSE

The constant step assumption simplifies the estimations, but produced a fairly good prediction of the overall route. This shows that the user may have actually walked constant strides for most of the processes. Towards the end, the user made a small turn, and this is well-reflected in the estimation, as shown in Figure 4.1a, proving that having more data makes CSE having an advantage at more detailed sections. However, at the corner turns, the changing angles of the estimation seemed to be bigger than the true angle, showing that the actual strides here may have been different. Overall, the method works well and is able to capture detailed data, but requires the constant step assumption to be well-satisfied.

4.1.2 ASE

Looking at Figure 4.1b, the calculated strides seems to work well, which shows a good distance performance at first steps and turnings. However, the small turn at the end of route is not reflected well. This is because as the unit now depends on steps rather than time unit, less data are available, and smaller details are omitted as a result. Furthermore, drifting still appears at the end, even though now increasing linearly instead of squared, proving that the method may not work well in the long run. Overall, the method works well for short estimations, but will not work well in small details and have small risk of drifting.

4.1.3 Heading estimation

With the ending position remains near the starting point, the heading estimation can be concluded to work quite well, as it reflected the turns well on either distance estimation methods. However, the heading when walking at the 3rd edge seems to slightly go off from the actual heading. Figure 3.1 shows that both gyroscope and magnetometer headings are higher than the actual orientation, making the Kalman Filter unable to get the correct heading as well. One possible cause is that the phone position is assumed to be constant, but during walking, slight tilts may happen in user's hand. Furthermore, with unknown magnetic sources, the magnetometer would still be very prone to disturbances, distracting the Kalman Filter estimation. In order to achieve a better result, the development sources need to have their own error corrected first.

4.2 Potential improvements & ideas

Overall, the methodologies above have performed well. While potential improvements exist, due to time constraint and limited resource, they remain to be ideas that can be saved for later development when the condition allows.

Extrapolation for ASE The main downfall of ASE is not having enough data, and wasted the existing data as a result. To be able to utilize this method for smaller changes, extrapolation can be done to approximate better displacements.

Gyroscope drift removal In literature, a variety of methods are developed to attempt and remove the drifting of gyroscope before inputting to Kalman Filter, such as fusion with other data sources [4], or build larger state vectors for the Kalman Filter [1]. However, most of them are complex to build, and may require additional time and resources in order to get the best estimation.

Dynamic magnetometer calibration Given that the remaining problem for magnetometer data is multiple flux disturbances, when more computation power and time allows, the data can be split into small sections, and calibration can be done separately on each batch.

4.3 Conclusion

Overall, the developed indoor GPS worked well, with the final result resembling the original walking route to an acceptable accuracy, eliminating the erroneous problem of outdoor GPS. The system is also proven to be simple to run, while requiring minimal number of user-defined parameters. However, to achieve better precision, more focus is needed to eliminate existing problems of data sources that contribute to the model, which includes accelerometer, magnetometer and gyroscope. The output tracking result will become meaningful for close-range tracking applications, such as developing path-finding algorithms or space mapping, or detecting a trajectory rule of an object of interest.

Bibliography

- [1] P Kaniewski and J Kazubek. Integrated system for heading determination. *Acta Phys. Pol. A.*, 116(3):325–330, September 2009.
- [2] Pengfei Guo, Haitao Qiu, Yunchun Yang, and Zhang Ren. The soft iron and hard iron calibration method using extended kalman filter for attitude and heading reference system. In *2008 IEEE/ION Position, Location and Navigation Symposium*. IEEE, 2008.
- [3] Rudolph Emil Kalman. A new approach to linear filtering and prediction problems. *Transactions of the ASME–Journal of Basic Engineering*, 82(Series D):35–45, 1960.
- [4] Shutong Li, Yanbin Gao, Gong Meng, Gang Wang, and Lianwu Guan. Accelerometer-based gyroscope drift compensation approach in a dual-axial stabilization platform. *Electronics*, 8(5), 2019.

Appendix A

Additional Resources

A.1 Linear Regression

Linear regression tries to fit a straight line in the form of $h(t) = \beta_0 + \beta_1 t$ through the given set of data points (x_i, y_i) . Let:

$$B = \begin{bmatrix} \beta_0 \\ \beta_1 \end{bmatrix} \quad X = \begin{bmatrix} 1 & x_0 \\ 1 & x_1 \\ \vdots & \vdots \\ 1 & x_n \end{bmatrix} \quad Y = \begin{bmatrix} y_0 \\ y_1 \\ \vdots \\ y_n \end{bmatrix}$$

To find β_0, β_1 , solve for $Y = XB$.

A.2 Acceleration Integration

Each step in the pedometer is represented as a peak with magnitude p and width w . It can be approximated by a sine wave in the form of $\sin(\frac{\pi}{w})$. By integrating the first half of the wave, the maximum velocity reached can be found.

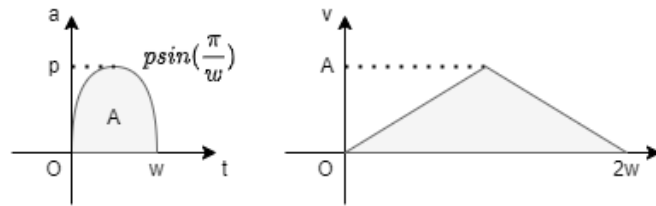


Figure A.1: Approximated shape of the signals of a step from accelerometer: the first half of acceleration and velocity

The area of the first half of sine wave can be done as follows:

$$A = \int_0^w p \sin\left(\frac{\pi}{w}x\right) dx = \left[-\frac{pw}{\pi} \cos\left(\frac{\pi}{w}x\right) \right]_0^w = \frac{pw}{\pi}$$

Then, the accumulated displacement can be calculated using the triangle area formula:

$$d = \frac{2wA}{2} = wA = \frac{pw^2}{\pi}$$

From this we can also see that p is linearly proportional to A - the retrieved speed. Therefore, the initial speed can also be approximated as $v_0 = \text{const} \times p$, where the user can adjust the constant parameter. For this task, the constant is set to 1.

A.3 Rotation Matrices

The 3D rotation matrix for rotation of θ around 1 axis can be denoted as follows:

$$\begin{bmatrix} \cos(\theta) & 0 & \sin(\theta) \\ 0 & 1 & 0 \\ -\sin(\theta) & 0 & \cos(\theta) \end{bmatrix} \quad \text{(y-axis rotation)}$$

$$\begin{bmatrix} \cos(\theta) & -\sin(\theta) & 0 \\ \sin(\theta) & \cos(\theta) & 0 \\ 0 & 0 & 1 \end{bmatrix} \quad \text{(z-axis rotation)}$$

To add up rotations, these rotation matrices can be multiplied sequentially.